6th NDT in Progress 2011
International Workshop of NDT Experts, Prague, 10-12 Oct 2011

Ground Penetrating Radar as tool for nondestructive evaluation of soil

Raimond GRIMBERG, Rozina STEIGMANN, Nicoleta IFTIMIE, Adriana SAVIN

National Institute of Research and Development for Technical Physics, Iasi, Romania

Abstract.
A major risk during the construction of highways, railways, civil and industrial buildings is represented by the existence in the soil of ammunition and unexploded mines. Supplementary, in localities, during the excavation, pipes, electrical cables, archaeological sites, the voids might be found. The modern method for their detection is Ground Penetrating Radar (GPR) which gives necessary information at the scanning of the surface to be examined. Due to the high frequency, the maximum depth at which the objects can be detected is limited to 4 - 4.5 m. In the same time, the radar-grams interpretation is quite complicate, requiring rich experience and a corresponding database. The obtained experimental data and some signal and image processing procedures are presented in this paper in order to make a correct evaluation of type of buried ammunitions, including antitank mines, as caliber, dimensions and their location in the horizontally plan as well in depth.

Keywords: GPR, UXO, signal, and image processing, shape recognition

1. Introduction

Ground Penetrating Radar (GPR) is a non-intrusive technique used to obtain information about the medium below the surface of the earth. The technique relies upon transmission of electromagnetic energy into the earth, and subsequent reflection of the energy at interfaces of differing dielectric permittivity. There are a wide range of domains that have used GPR such as archaeology, geology, civil engineering, and military applications. Current applications of GPR include but are not limited to detection of unexploded ordnance (UXO), buried landmines (anti-personnel and anti-tank), road layer thickness measurements, position of underground pipes and cables.
To operate successfully GPR must achieve [1] an adequate signal to clutter ratio; an adequate signal to noise ratio; an adequate spatial resolution of the target and an adequate depth resolution of the target. Most GPR systems detect the backscattered signal from the target, although forward transmission methods are used in borehole tomography radar imaging [2]. When a down-looking antenna is scanned over a relatively small target, a characteristic hyperbolic arc appears in the time-domain data.
However, a significant limitation of GPR in this application is that it can be very difficult for a non-expert user to extract information about the underground from the raw data.

2. GPR principles

A block diagram of a generic GPR system is shown in Figure 1.
The transmitter can provide an amplitude frequency or phase modulated waveform signal and the selection of the bandwidth, repetition rate or mean power will depend upon the path loss and target dimensions. The transmit (Tx) and receive (Rx) antennas will be usually identical and will be elected to meet the characteristics of the generated waveform.
The majority of GPR systems uses an impulse time domain waveform and receives the reflected signal in a sampling receiver.
The key of success of this method lies in proper pre-processing of the GPR data, which is a very important step before formal data analysis can begin.

Models of the GPR situation range from a simple single frequency evaluation of path losses to complete 3D time domain descriptions of the GPR and its environment. Modeling techniques include single frequency models, time domain models, ray tracing, integral techniques and discrete element methods. The Finite Difference Time Domain (FDTD) technique has become one of the popular techniques [1], [3].

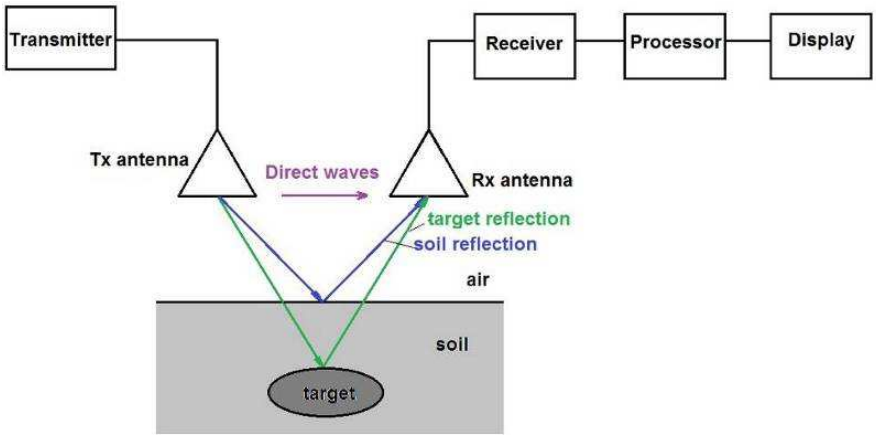

Figure 1. Block diagram of a generic GPR system.

3. The equipment and the studied samples

The GPR equipment is Utility Scan - Standard System - GSSI – USA, having 400MHz antenna. On the front wheel the GPR displacing system is mounted an encoder that assures the determination of the position with 1mm precision. The sampling raster is 0.04ns, the quantization being made on 16bits.
An experimental test site has been arranged on a terrain from which metallic objects (the detection was effectuated with GPR), civil engineering materials and big stones have been removed. In this test site, parallelepiped holes with $1x1x0.8m^3$ dimensions have been practiced, where different types of ammunition (without explosive material). The ammunitions studied are presented in Figure 2.

Figure 2. The ammunition tested

After its introduction in the hole, this was tamped with soil which has been pressed.
In Figure 3 is presented the GPR equipment in the test site.

The average value of dielectric permittivity of the soil was determined during the measurements, using standard procedures [4] as being 6. Each situation has been individually simulated using GPRMax2D, based of FTDT method [3].

Figure 3. The GPR system in the test site

4. Signal processing

Figure 4 present the scan #19 which represents the passing over a zone in which a Kargo projectile (122mm caliber, 780mm length) was buried in horizontally position (a) and the result obtained by simulation (b). It can be observed that in the case of real measurements, the image is very noisy, containing, in addition, clutters. Using the specific technology of ultrasound examinations, the image form figure 4a is a B-scan made from 55 raw data A-scan type.

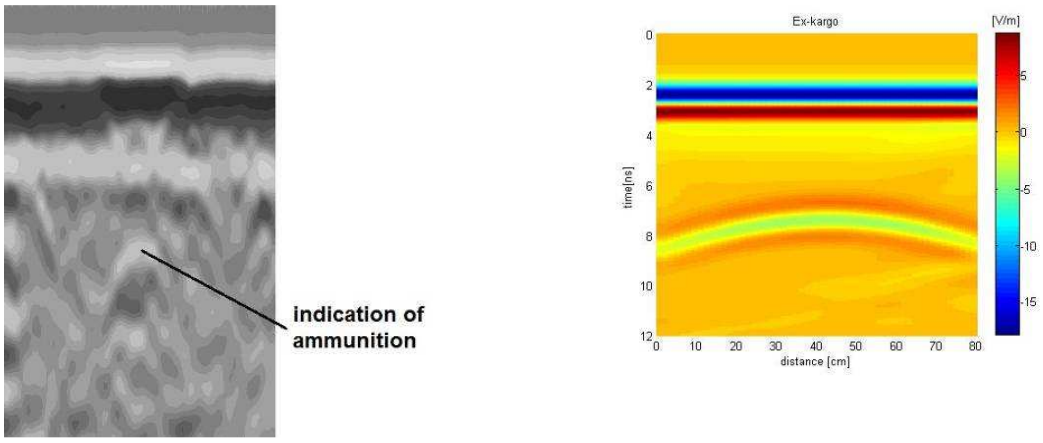

a b

Figure 4. Scan of Kargo projectile: a) raw data; b) simulation using GPRMAX 2D.

4.1. A-scan processing

An important process operation is to ensure that the mean value of the A-scan is near to zero. This assumes that the amplitude probability distribution of the A-scan is symmetric about the mean value.

$$A'_n = A_n - \frac{1}{N}\sum_{n=1}^{N} A_n \tag{1}$$

where A_n -unprocessed data sample, A'_n - processed data sample, n – the sample number, N – total number of samples.
A next step in GPR signal processing is noise reduction and can be achieved by either averaging each individual sample at the A-scan. The general effect is to reduce the variance of the white noise and gives an improvement in signal to noise ratio.
The general form of the filtering operation is given by

$$A'_n = A_n + \frac{A_n - A'_{n-1}}{K} \tag{2}$$

where A'_n is averaged value, A_n is the current value.
The factor K may be chosen to be related to n, N, or a fixed value, which will weigh the averaged value appropriately. Averaging has no effect on clutter.

4.2. B-scan processing

If we consider an assembly set of five samples comprising a B-scan, there are a number of approaches to signal processing which can be considered. Imaging with GPR data is frequently hampered by clutter.
The principal problem for a correct interpretation of GPR images consists in the extraction of unwanted signals as the ones due to transmission of forward wave from Tx to Tr and those due to reflection on the air-soil interface. This operation is named background removal, a series of specific algorithms being used. The results, good enough, have been obtained using the simple procedure named subtract mean trace [5].
In this method, we define a window of L pixels and subtract from all the pixels in this window the mean of the pixels in it. The window is moved along and the procedure is repeated until the entire image is covered, as following

$$g(x,y) = f(x,y) - \frac{1}{L}\sum_{i=-\frac{L}{2}}^{i=\frac{L}{2}} f(x+i,y) \tag{3}$$

where g – filtered image, f- raw data and L is the window size.
This method works well, even with GPR data taken over soil having an uneven profile, provided the magnitude of the ground reflection is uniform across the GPR map. Because of the factors such as variations in soil moisture content, vegetation, soli profile, etc., the method of subtract mean trace is often unsatisfactory in practice. We propose a method in which spatial variations in both the ground reflection magnitude and delay are simultaneously estimate using nonlinear optimization. Because these variations are relatively smooth functions of position, we model them using low-order polynomials.
To proceed, the measured data are split into N_{seg} spatial segments. Over each segment we approximate the spatial resolution in both the amplitude and time delay of the ground reflection by weighted sums of Chebyshev polynomials, the domain of the segment was normalized to the interval [-1,1].
Let $A_i(x)$ denotes the spatially ground reflection amplitude and $B_i(x)$ the time delay of the ground reflection peak over segment i^{th}. We approximate $A_i(x)$ and $B_i(x)$ as a sum

$$A_i(x) = \sum_{n=0}^{4} a_{i_n} T_n(x)$$
$$B_i(x) = \sum_{n=0}^{4} b_{i_n} T_n(x) \tag{4}$$

where $T_n(x)$ are the Chebyshev polynomials defined by the recursive relation

$$T_{n+1}(x) = 2T_n(x) - T_{n-1}(x), \qquad n > 1 \tag{5}$$

with $T_0(x)=1$ and $T_1(x)=x$.
Because the reflection coefficient at the air-soil interface is typically complex, we can represent the coefficients as

$$\bar{a}_i = \left[a_{i_0}^{real}, \quad a_{i_0}^{imag}, \quad a_{i_1}^{real}, \quad a_{i_1}^{imag}, \quad \ldots \right] \tag{6}$$

$$\bar{b}_i = \left[b_{i_0}, \quad b_{i_1}, \quad \ldots \right] \tag{7}$$

The frequency-domain ground reflection in spatial segment i[th] can be estimate as

$$G_i^{est}(x, f) = A_i(x) H(f) \exp\left(-2\pi j f B_i(x)\right) \tag{8}$$

where $H(f)$ is the windowed frequency response of the radar, i.e.

$$H(f) = \bar{H}(f) W(f) \tag{9}$$

In which $\bar{H}(f)$ is the average frequency spectrum of the raw GPR data within the segment and $W(f)$ is a window applied when creating the time-domain data. We have used a Hanning window. The time domain reflection estimated becomes

$$g_i^{est}\left(x, t, \bar{a}_i, \bar{b}_i\right) = A_i(x) h\left(t - B_i(x)\right) \tag{10}$$

Where *h(t)* is the inverse Fourier transform of $\mathrm{H(f)}$. The measured ground reflection over segment i^{th} can be expressed as

$$g_i^{meas}(x,t) = g_i^{est}\left(x, t, \bar{a}_i, \bar{b}_i\right) + n_i(x,t) \tag{11}$$

where $n_i(x,t)$ represents the modeling error. The coefficients $\bar{a}_i$ and $\bar{b}_i$ are found by a least-square error process, which requires a nonlinear optimization of

$$\left[\hat{a}_i, \hat{b}_i \right] = \arg\left(\min \left\| g_i^{meas}(x,t) - g_i^{est}\left(x, t, \bar{a}_i, \bar{b}_i\right) \right\|^2 \right) \tag{12}$$

Once the weighting coefficients $\bar{a}_i$ and $\bar{b}_i$ are estimated, the amplitude term $A_i(x)$ and the delay $B_i(x)$ of segment i^{th} are evaluated using (4).

Parameter estimation was performed using a nonlinear least square error minimization function, in the Matlab 2009b Optimization Toolbox. If the optimization routine not converges for a data set, we must use a recursive approach.
Imaging techniques can be used to focus the energy present in a point target's hyperbolic arc back to a single point.
This technique, named migration allows the determination of the depths of buried objects.

5. Results

The GPR raw data for different types of UXO, presented in Figure 2, have been obtained. All types of UXO have been buried at 0.8m depth, excepting the antitank plastic mine that was buried at 0.6m, according to its indications for using it.
Also, groups of different types of UXO have been used. The measurement conditions had remain the same in all cases: 0.05m distance between row data in A-scan, 1024 samples/cm, 0.1m distance between successive B-scans, 20dB amplification.
The signal processing methods and their efficacy are presented in Figure 5, corresponding to the scan #19 from Figure 4, including the procedures of A-scan processing described in chapter 3.1. In Figure 5a it is presented the background removal effect applied to original image from Figure 4a.

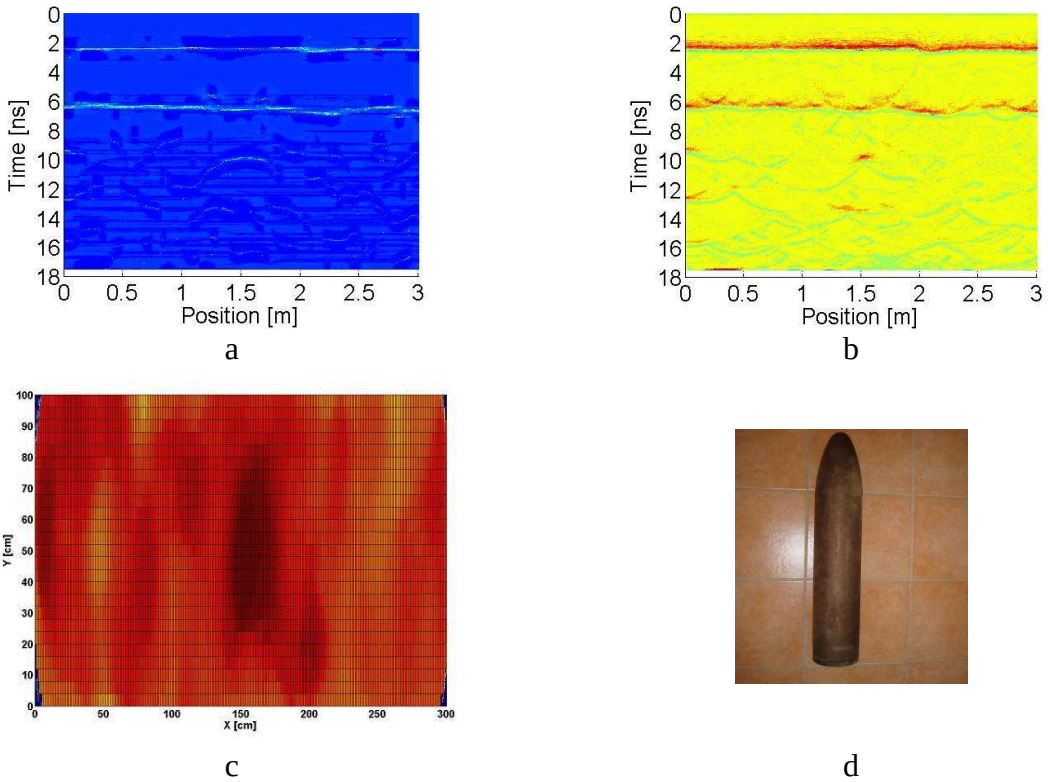

Figure 5. GPR images of Kargo projectile: a) after A-scan processing and ground removal; b) after migration; c) top view; d) photo of the Kargo projectile

After applying migration technique, the region of maximum concentration of energy, corresponding to the real position of top surface of the Kargo projectile has been emphasized. It can be observed that the migration procedure locates correct the superior part of the projectile. Concatening the B-scan obtained after migration of corresponding GPR images of

the Kargo projectile and applying top view technique, the image of the Kargo is obtained and from simple measurements, the type and the dimensions of the projectile can be determined. Also, the depth at which the projectile has been buried can be determined from raw data after migration.
The same techniques have been used for detection and evaluation of two projectiles (Figure 6a), type 76mm caliber, the distance between their generatrix being 0.6m (Figure 6b). The top view for an antitank mine MAT 62B (Figure 6c) is presented in Figure 6d. It must be mentioned that its shell is made from plastic, the metallic parts having a total weight of 15.8g.

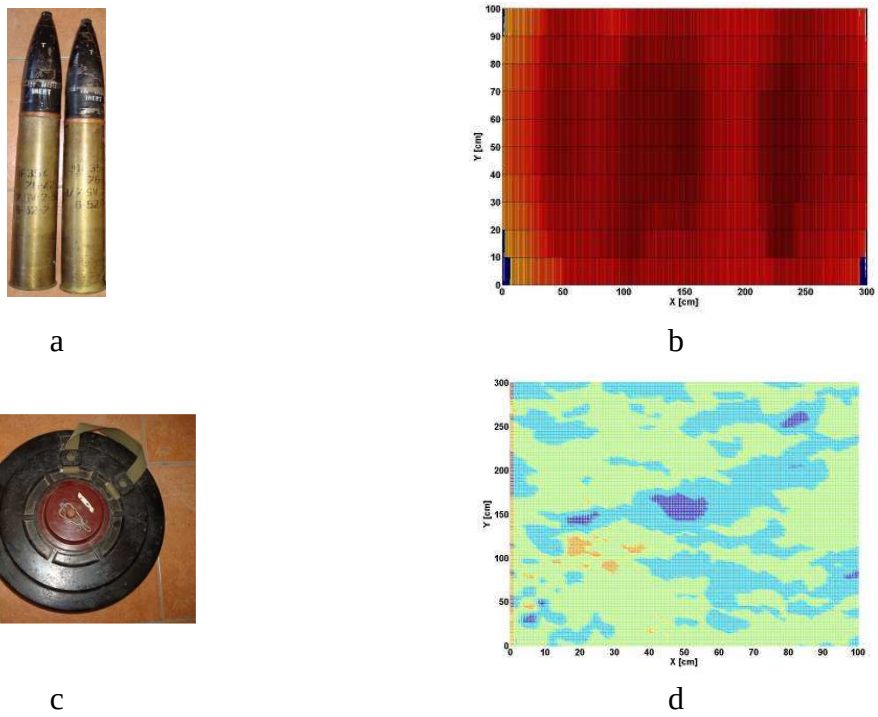

a b

c d

Figure 6. a) Photo of two projectile, 76mm caliber; b) Top view of GPR processed data for the two projectile; c) Photo of antitank mine; d) Top view of GPR processed data for the antitank mine

6. Conclusions

GPR has started to be used, with good results, in different types of application, from which, UXO must be nominated. This fact is more important for the countries that have been theatre of war. To can interpret correct the images delivered by GPR, due to the high level of noise and of clutters, it is very important to solve the forward problem using FDTD procedure. Applying specific procedures of signal and image processing, the shape of UXO become visible, the type, caliber, number and their coordinate can be determined from simple measurements on the results. These procedures allow the emphasizing of antitank mines from plastic, even if the weight of metallic parts is very small.

7. Acknowledgements

Special thanks to the Colonel Stefan Lazar, former Chief Inspector of Inspectorate for Emergency Situations “Mihail Grigore Sturdza” Iasi, Romania.
This paper is partially supported by the Romanian Ministry of Education, Research and

Innovation under PN II Program – Project 32-134/2008 SysArr and Bilateral Project MENDE Ro-Sk/2011.

References

1. D.J.Daniels, ‘Ground Penetrating Radar’ 2nd ed., , IEE 2004, UK.
2. M.J.g Yi, J.H. Kim, S.J.Cho, M. Sato, ‘Integrated Application of Borehole Radar Reflectionand Resistivity Tomography to Delineate Fractures at a Granite Quarry’, *Subsurface Sensing Technologies and Applications, Vol. 6, No. 1, January 2005*
3. A.Giannopoulos ‘GprMax2D/3D, User's Guide’ 2003
4. ISO11265:1994 – Soil quality, Determination of specific electrical conductivity
5. C.C.Chen, J.D.Young, L.Peters, F.Paynter, ‘Radar signature measurements of buried, unexploded ordnance targets’, Tech.Rep. 727388-2, The Ohio State University, Electroscience Laboratory, Columbus, Ohio, 1994.